Supplementary Material

Crosstalk between the gut microbiota and monocyte-like macrophages mediates an inflammatory response to promote colitis-associated tumorigenesis

Supplementary Methods

Flow cytometry, colonic epithelial cell preparation, and *in vitro* experiments

Colonic tissue was opened longitudinally and washed with PBS. Then, tissue was cut into 0.5 cm pieces and incubated in 5 mM EDTA and 1 mM DTT solution for 30 minutes at 37 degrees. After vigorous stirring, supernatants from incubation were centrifuged and resuspended in PBS. Colonic epithelial cells (CECs) were isolated using EPCAM microbeads (Miltenyi) according to the manufacturer's instructions. For qPCR experiments, CECs were treated for 6 hours with varying concentrations of LPS (Solarbio). Fecal extracts were prepared as described previously.[1, 2] Briefly, feces pooled from 5 mice from the antibiotic (ABX)-treated or untreated AOM-DSS mice group were suspended in PBS (100 mg/ml), homogenized, centrifuged and filtered to remove aggregates. For intracellular cytokine staining assays, CECs were stimulated for 5 hours with fecal extracts in the presence of Brefeldin A (BioLegend) and Monensin Solution (BioLegend). Subsequently, cells were stained with an antibody against EPCAM (clone G8.8, BioLegend) and fixed, permeabilized using fixation/permeabilization buffers (BioLegend), followed by staining intracellularly for CCL2 (clone 2H5, BioLegend). In some experiments, CEC culture was stimulated with fecal extracts in the presence of TLR4 inhibitor (TAK-242, 100 nM; MedChemExpress) added 30 minutes before stimulation. Fecal LPS levels were quantified using a mouse LPS ELISA kit (CUSABIO) according to the manufacturer's protocol.[3]

For specifically isolating LP mononuclear cells (LPMCs), the remaining intestinal pieces after EDTA incubation were cut into 1 mm pieces, and digested with type IV collagenase (1 mg/ml, Sigma-Aldrich) for 1 hour at 37 degrees. After filtration, isolated colonic LPMCs were resuspended in FACS buffer and blocked the Fc-receptors with an anti-CD16/CD32 mAb (BioLegend). Cells were stained with antibodies directed against CD45 (clone 30-F11, BioLegend), CD11b (clone M1/70, BioLegend), F4/80 (clone BM8, BioLegend), Siglec-F (clone 1RNM44N, eBioscience), CD11c (clone N418, BioLegend), MHC-II (clone AF6-120.1,

BioLegend), Ly6C (clone HK1.4, BioLegend), Gr-1 (clone RB6-8C5, BioLegend), TNF-α (clone MP6-XT22, BioLegend), IL-1 beta Pro-form (clone NJTEN3, eBioscience), CD206 (clone C068C2, BioLegend), Ki-67 (clone 16A8, BioLegend), IL-17A (clone TC11-18H10.1, BioLegend), CD4 (clone GK1.5, BioLegend), CX3CR1 (clone SA011F11, BioLegend), CD135 (clone A2F10, BioLegend), CD115 (clone AFS98, BioLegend), CCR2 (clone 475301, R&D Systems), CCR3 (clone REA122, Miltenyi Biotec), CCR4 (clone 2G12, BioLegend), CCR5 (clone REA354, Miltenyi Biotec), CCR6 (clone REA277, Miltenyi Biotec), CCR8 (clone REA921, Miltenyi Biotec), CXCR4 (clone REA107, Miltenyi Biotec). Zombie Red™ Fixable Viability Kit (BioLegend) was used as a viability stain. Flow cytometry was performed on the CytoFLEX S flow cytometer (Beckman Coulter). CytExpert software was used for data analysis.

Intracellular cytokine staining is a leading technique for visualizing cellular immune respons, which can be helpful to detect cytokine production at the single-cell level. However, the presence of intracellular cytokine does not fully equate to what happens *in vivo*. In some experiments, colonic macrophages were isolated using Anti-F4/80 Microbeads UltraPure (Miltenyi) from mice at different stages of tumorigenesis (AOM-DSS baseline/wk3/wk6/wk9). To further evaluate the macrophage cytokine responses *in vivo*, mice were induced by intrarectal administration of 0.25 mg Brefeldin A. Colonic tissue was harvested 6 hours after Brefeldin A instillation, and flow cytometric analysis of intracellular cytokine levels was performed.

In select experiments, colonic MLMs were sorted by BD FACSAria II cell sorter system (BD Biosciences). Sorted colonic MLMs (1×10^5 cells) were cultured in the presence of LPS (1μg/ml; Solarbio), or a combination of TLR4 inhibitor (TAK-242, 1μM; MedChemExpress)/COX-2 inhibitor (Celecoxib, 10μM; Aladdin). After 36 hours, supernatants from MLM-drug cocultures were harvested. Sorted splenic $CD4^+$ cells (1×10^5 cells) using CD4 microbeads (Miltenyi) were treated with anti-CD3 (BioLegend) plus anti-CD28 (BioLegend) Abs in the presence of 1 ng/ml TGF-β (Peprotech), 20 ng/ml IL-6 (Peprotech). Supernatants from MLM-drug cocultures were added to the culture on day 0. As indicated, anti-mouse IL-1β (10μg/ml; Bioxcell) was added in medium unless mentioned. Three days after treatment, cells were restimulated with Cell Stimulation Cocktail (eBioscience) before intracellular staining of cytokines.

Bacterial DNA quantification, sequencing and analysis

Stool bacterial load was quantified using Bacteria Quantitative PCR Kit (TaKaRa). The V3–V4 region of 16S rRNA genes was amplified using 341F (CCTAYGGGRBGCASCAG) and 806R (GGACTACNNGGGTATCTAAT) primers. PCR reactions were conducted in 30 μL reactions with 15 μL of Phusion® High-Fidelity PCR Master Mix (New England Biolabs); 0.2 μM of forward and reverse primers, and about 10 ng template DNA. Sequencing libraries were generated using Ion Plus Fragment Library Kit 48 rxns (Thermo Scientific) following manufacturer's recommendations. The quality of library was evaluated by the Qubit@ 2.0 Fluorometer (Thermo Scientific). At last, the library was sequenced on an Ion S5™ XL platform. After data split, filtration and chimera removal, sequence analysis was performed by Uparse software.[4] Sequences with ≥97% similarity were assigned to the same OTUs. For each representative sequence, the Silva Database (https://www.arb-silva.de/) was used based on Mothur algorithm to annotate taxonomic information.[5] Metastats software was used to determine differences in the abundances of individual taxonomy between the two groups.[6] LEfSe was utilized for the quantitative analysis of biomarkers within different groups.[7]

Human studies

To determine species differences between patients with ulcerative colitis (UC) or colorectal cancer (CRC) and healthy controls, curated human gut metagenomic data were downloaded from GMrepo database.[8] GMrepo is considered as one of the largest databases with enormous numbers of samples collected from 253 projects and 92 phenotypes, which is achieved by carefully curating meta-data and applying stringent criteria to keep only high quality data. To further ensure the quality of the meta-data, manual curation was performed. The exclusion criteria were defined as follows: repeated sequencing run data corresponded to the same sample, a history of fecal microbiota transplantation or CRC. The list of enrolled human gut metagenomic runs is provided in **Supplementary Table 2** (collection date: 2020.7).

For integration of multiple microarray data sets, raw microarray data (.CEL files) were downloaded from the National Center for Biotechnology Information Gene Expression Omnibus (GEO, http://www.ncbi.nlm.nih.gov/geo), and pre-processed via the affy package. To minimize variations caused by different platforms, only samples probed with Affymetrix HT HG-U133+ PM (HT_HG-U133_Plus_PM) Array were

selected. The arrayQualityMetrics package was subsequently used to filter bad arrays, improving the quality of the experiments.[9] After background correction and normalization using Robust Multi-array Average, the inSilicoMerging package was applied to remove the batch effects and merge data sets from different sources.[10] PCA and hierarchical cluster analysis were carried out to validate the batch adjusted data. A total cohort of 194 human samples including 24 normal colonic tissues, 159 UC and 11 ulcerative colitis with neoplasia (UCN) tissues were enrolled, and the final list of the included samples is shown in **Supplementary Table 3**. Of the patients with UCN, four had low-grade dysplasia (LGD), three had high-grade dysplasia (HGD), and four had adenocarcinomas.[11] To determine differentially expressed genes (DEGs) in diseased samples, the limma package was used.[12] To obtain an overview of which biological processes were overrepresented in colitis-associated tumorigenesis, we performed gene ontology (GO) enrichment analysis with stringent criteria of adjusted p-value<1.0E-9 and pathway sets that annotate fewer than 300 genes to avoid very general sets.[13] GO terms were grouped according to semantic similarity.[14] We used limma-generated fold change values as the input data for subsequent Gene Set Enrichment Analysis (GSEA) analysis. GSEA was performed using the clusterProfiler package, together with the version 7.0 annotated gene sets (C2, C5 and C7) downloaded from the the Molecular Signature Database (MSigDB).[15] According to gene set variation analysis (GSVA) scores, top 10 gene sets were selected for each group.[16]

Tissue-infiltrating immune cells were determined using “Cell type Identification By Estimating Relative Subsets Of RNA Transcripts (CIBERSORT)” algorithm, based on the predefined LM22 signature.[17] LM22 is a validated gene signature matrix of 547 marker genes on 22 immune cell subtypes. For example, the unique expression pattern of M0-M2 macrophage genes recapitulates the phylogeny of macrophages according to their differentiation, and it contains significantly DEGs identified by comparing each cell subset with all other populations.[18, 19] All these DEGs used to form LM22 are provided in the CIBERSORT web portal (http:// cibersort.stanford.edu/).

References

1 Bhattacharya N, Yuan R, Prestwood TR, *et al.* Normalizing Microbiota-Induced Retinoic Acid Deficiency Stimulates Protective CD8(+) T Cell-Mediated Immunity in Colorectal Cancer. *Immunity* 2016;**45**:641-55.doi:10.1016/j.immuni.2016.08.008

2 Seo SU, Kamada N, Munoz-Planillo R, *et al.* Distinct Commensals Induce Interleukin-1beta via NLRP3 Inflammasome in Inflammatory Monocytes to Promote Intestinal Inflammation in Response to Injury. *Immunity* 2015;**42**:744-55.doi:10.1016/j.immuni.2015.03.004

3 Qian G, Jiang W, Zou B, *et al.* LPS inactivation by a host lipase allows lung epithelial cell sensitization for allergic asthma. *J Exp Med* 2018;**215**:2397-412.doi:10.1084/jem.20172225

4 Edgar RC. UPARSE: highly accurate OTU sequences from microbial amplicon reads. *Nat Methods* 2013;**10**:996-8.doi:10.1038/nmeth.2604

5 Quast C, Pruesse E, Yilmaz P, *et al.* The SILVA ribosomal RNA gene database project: improved data processing and web-based tools. *Nucleic Acids Res* 2013;**41**:D590-6.doi:10.1093/nar/gks1219

6 Foster EK. METASTATS: behavioral science statistics for Microsoft Windows and the HP49G programmable calculator. *Behav Res Methods Instrum Comput* 2003;**35**:325-8.doi:10.3758/bf03202560

7 Segata N, Izard J, Waldron L, *et al.* Metagenomic biomarker discovery and explanation. *Genome Biol* 2011;**12**:R60.doi:10.1186/gb-2011-12-6-r60

8 Wu S, Sun C, Li Y, *et al.* GMrepo: a database of curated and consistently annotated human gut metagenomes. *Nucleic Acids Res* 2019.doi:10.1093/nar/gkz764

9 Kauffmann A, Gentleman R, Huber W. arrayQualityMetrics--a bioconductor package for quality assessment of microarray data. *Bioinformatics* 2009;**25**:415-6.doi:10.1093/bioinformatics/btn647

10 Taminau J, Meganck S, Lazar C, *et al.* Unlocking the potential of publicly available microarray data using inSilicoDb and inSilicoMerging R/Bioconductor packages. *BMC Bioinformatics* 2012;**13**:335.doi:10.1186/1471-2105-13-335

11 Pekow J, Dougherty U, Huang Y, *et al.* Gene signature distinguishes patients with chronic ulcerative colitis harboring remote neoplastic lesions. *Inflamm Bowel Dis* 2013;**19**:461-70.doi:10.1097/MIB.0b013e3182802bac

12 Ritchie ME, Phipson B, Wu D, *et al.* limma powers differential expression analyses for RNA-sequencing and microarray studies. *Nucleic Acids Res* 2015;**43**:e47.doi:10.1093/nar/gkv007

13 Northcott PA, Buchhalter I, Morrissy AS, *et al.* The whole-genome landscape of medulloblastoma subtypes. *Nature* 2017;**547**:311-7.doi:10.1038/nature22973

14 Yu G, Li F, Qin Y, *et al.* GOSemSim: an R package for measuring semantic similarity among GO terms and gene products. *Bioinformatics* 2010;**26**:976-8.doi:10.1093/bioinformatics/btq064

15 Yu G, Wang LG, Han Y, *et al.* clusterProfiler: an R package for comparing biological themes among gene clusters. *OMICS* 2012;**16**:284-7.doi:10.1089/omi.2011.0118

16 Hanzelmann S, Castelo R, Guinney J. GSVA: gene set variation analysis for microarray and RNA-seq data. *BMC Bioinformatics* 2013;**14**:7.doi:10.1186/1471-2105-14-7

17 Newman AM, Liu CL, Green MR, *et al.* Robust enumeration of cell subsets from tissue expression profiles. *Nat Methods* 2015;**12**:453-7.doi:10.1038/nmeth.3337

18 Abbas AR, Baldwin D, Ma Y, *et al.* Immune response in silico (IRIS): immune-specific genes identified from a compendium of microarray expression data. *Genes Immun* 2005;**6**:319-31.doi:10.1038/sj.gene.6364173

19 Cho HJ, Shashkin P, Gleissner CA, *et al.* Induction of dendritic cell-like phenotype in macrophages during foam cell formation. *Physiol Genomics* 2007;**29**:149-60.doi:10.1152/physiolgenomics.00051.2006

Supplementary Figures and Tables

Supplemental Figure 1

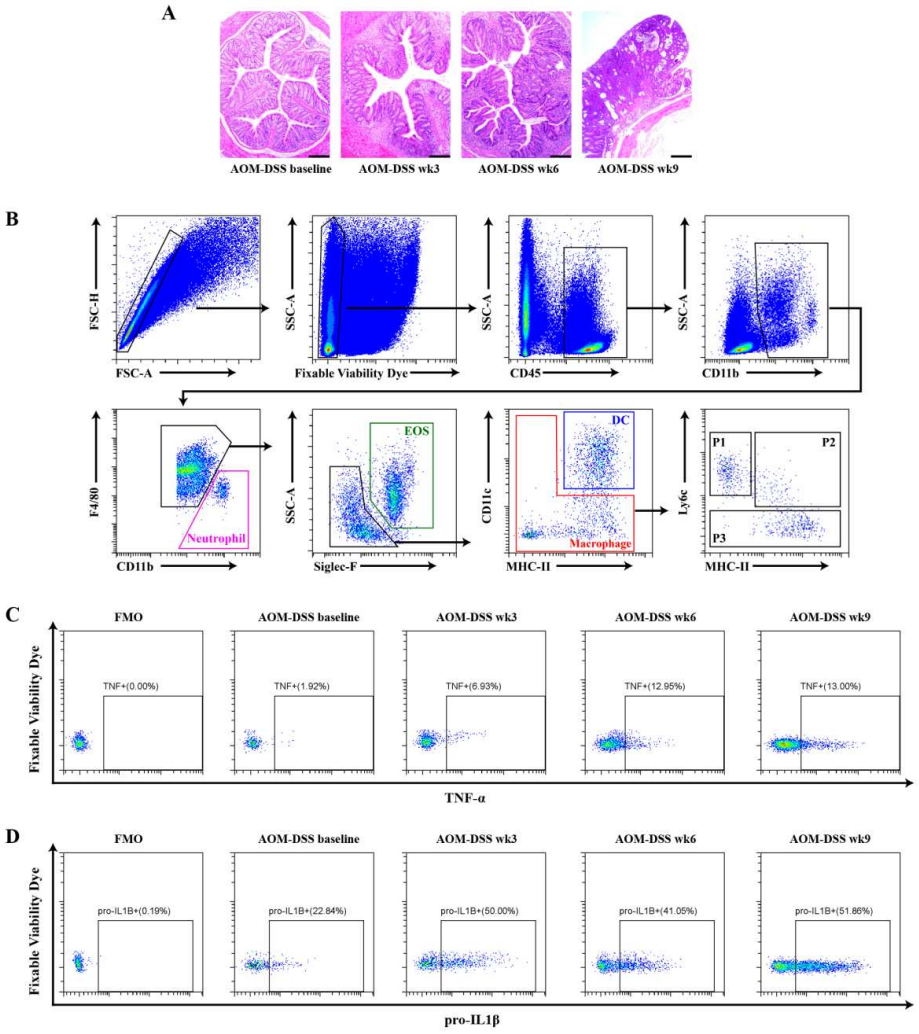

Supplemental Figure 1: Temporal analysis of alterations in colonic macrophages during murine colitis-associated tumor formation.

(A) Representative hematoxylin eosin-staining images in the AOM-DSS model throughout disease progression (scale bar, 200 μm). (B) Gating strategy used to identify macrophage subsets amongst colon digests. (C-D) Representative flow cytometry plots of intracellular TNF-α (C) and pro-IL1β (D) staining in colonic macrophage. The percentage of positive cells for each marker was determined based on fluorescence minus one (FMO) control.

Supplemental Figure 2

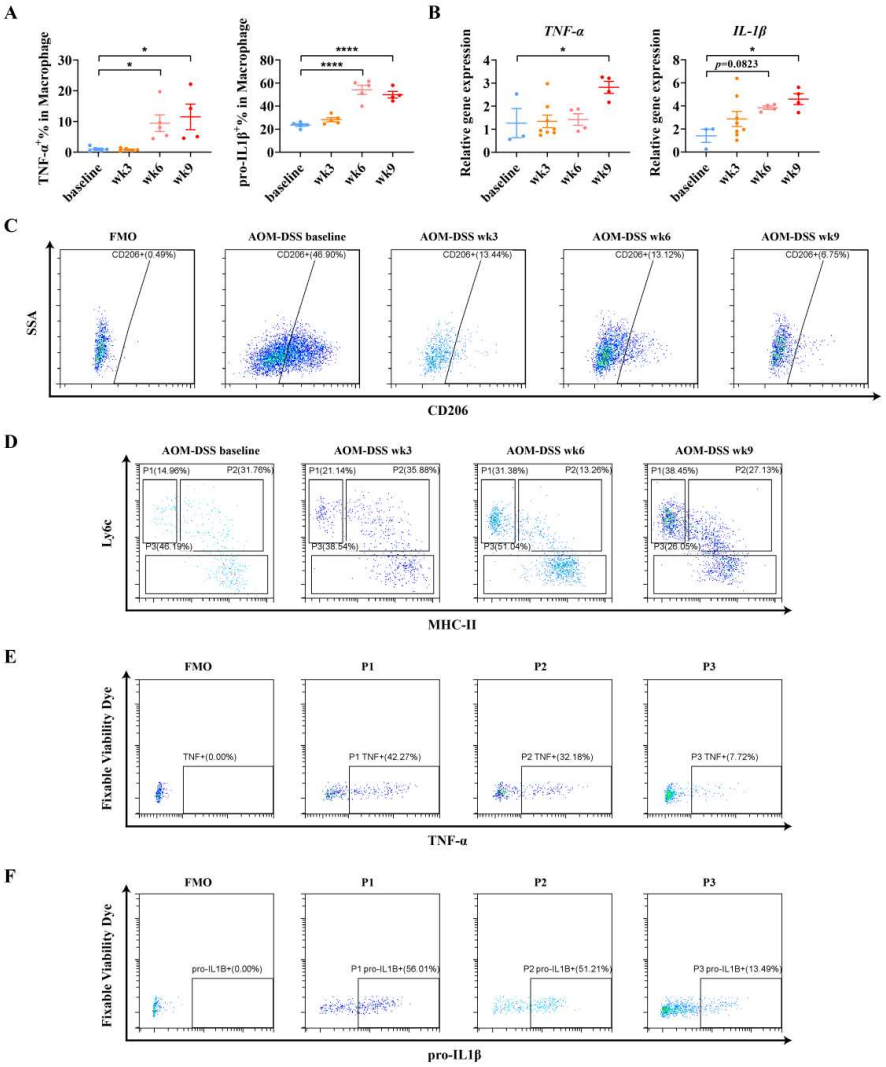

Supplemental Figure 2: Colonic MLM accumulation precedes tumor formation with a potent inflammatory cytokine-producing ability.

(A) TNF-α and pro-IL1β levels of colonic macrophage were measured from mice with intrarectal injection of Brefeldin A (AOM-DSS baseline/wk3/wk6/wk9: n = 5/5/5/4). p<0.05 = *; p<0.0001 = ****, one-way ANOVA. (B) *TNF-α and IL-1β* levels in sorted colonic macrophages (AOM-DSS baseline/wk3/wk6/wk9: n = 3/8/4/4). p<0.05 = *, one-way ANOVA. (C) Representative flow cytometry plots of CD206 expression in colonic macrophage. (D) Representative flow cytometry plots of three macrophage subsets at different time points. (E-F) Representative flow cytometry plots of intracellular TNF-α (E) and pro-IL1β (F) expression in each macrophage subset in mice of 9 weeks after AOM-DSS induction.

Supplemental Figure 3

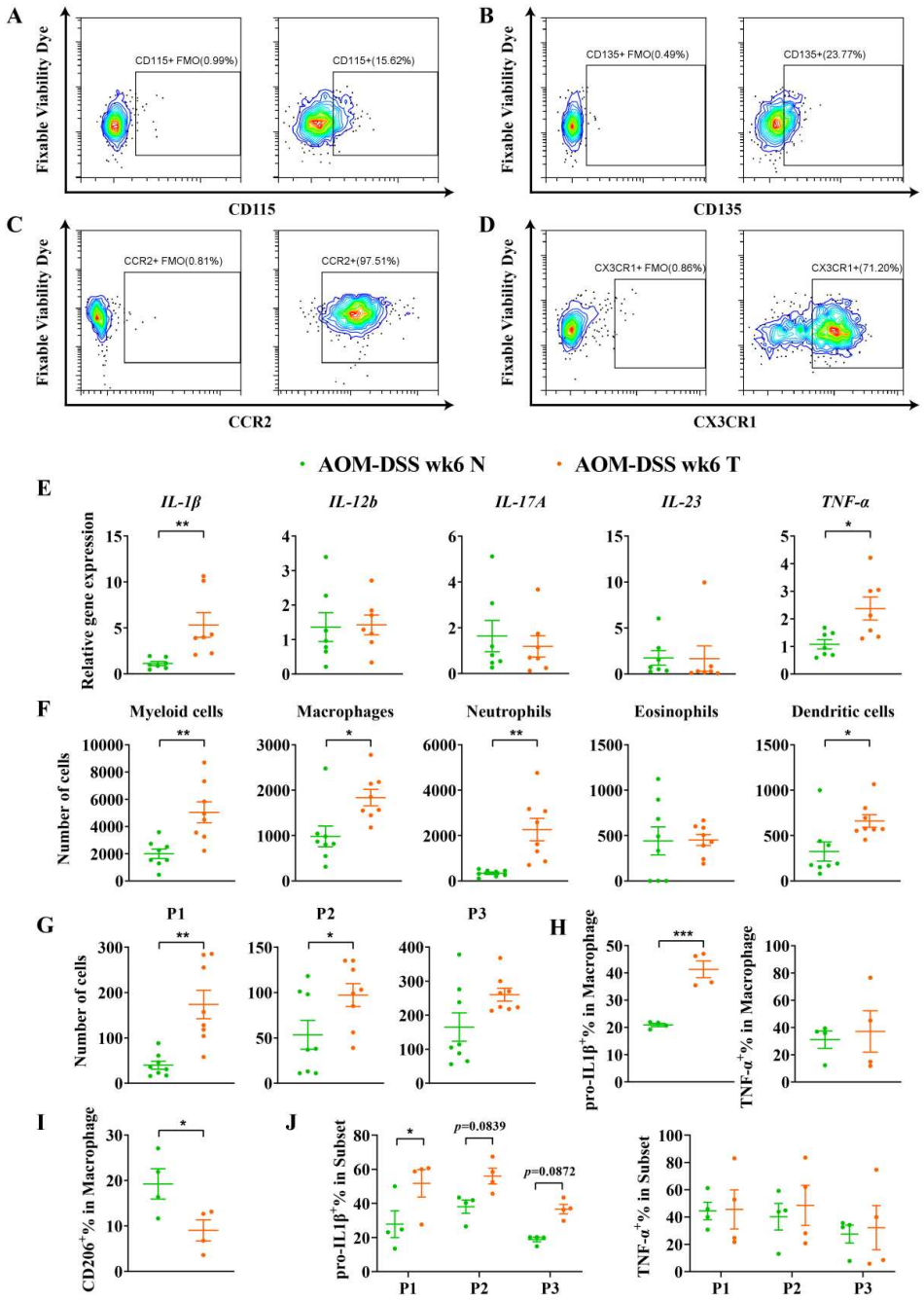

Supplemental Figure 3: Colonic MLM accumulation in the tumor site.

(A-D) Surface expression of CD115 (A), Flt3 (CD135) (B), CCR2 (C) and CX3CR1 (D) gated on live MLMs. (E-J) The difference in pro-inflammatory markers, myeloid cell subsets and macrophage dynamics between normal adjacent (N) and tumor (T) tissues in mice 6 weeks after AOM-DSS induction. (E) Normalized gene expression

of inflammation-related genes (n = 7 for each group). (F) Absolute cell numbers of myeloid cells and distinct myeloid cell subpopulations (n = 8 for each group). (G) Absolute cell numbers of each macrophage subset (n = 8 for each group). (H) Intracellular pro-IL1β and TNF-α levels in colonic macrophage (n = 4 for each group). (I) CD206 expression in colonic macrophages (n = 4 for each group). (J) Intracellular TNF-α and pro-IL1β levels in macrophage subsets (n = 4 for each group). Data are represented as mean ± SEM; $p<0.05$ = *; $p<0.01$ = **; $p<0.001$ = ***, student's t test (E-I), two-way ANOVA (J).

Supplemental Figure 4

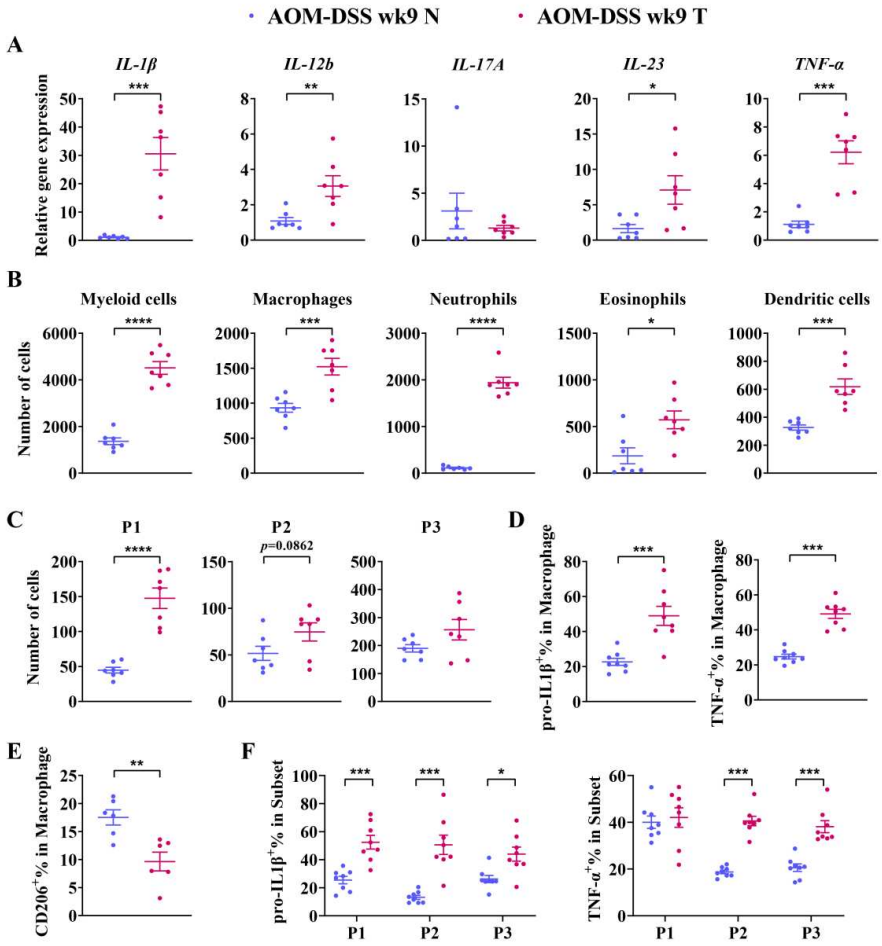

Supplemental Figure 4: Colonic MLM accumulation in the tumor site.

(A-F) The difference in pro-inflammatory markers, myeloid cell subsets and macrophage dynamics between normal adjacent (N) and tumor (T) tissues in mice 9 weeks after AOM-DSS induction. (A) Normalized gene expression of inflammation-related genes (n = 7 for each group). (B) Absolute cell numbers of myeloid cells and distinct myeloid cell subpopulations (n = 7 for each group). (C) Absolute cell numbers of each macrophage subset (n = 7 for each group). (D) Intracellular pro-IL1β and TNF-α levels in colonic macrophage (n = 8 for each group). (E) CD206 expression in colonic macrophages (n = 6 for each group). (F) Intracellular TNF-α and pro-IL1β levels in macrophage subsets (n = 8 for each group). Data are represented as mean ± SEM; p<0.05 = *; p<0.01 = **; p<0.001 = ***; p<0.0001 = ****, student's t test (A-E), two-way ANOVA (F).

Supplemental Figure 5

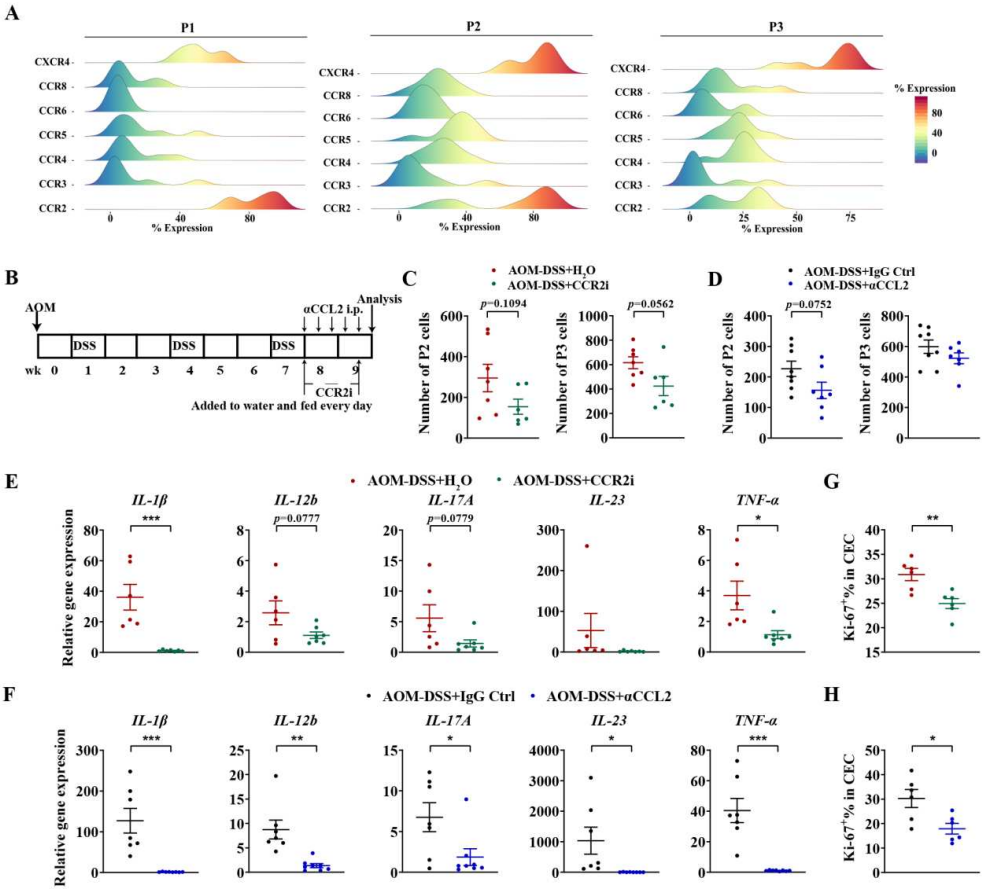

Supplemental Figure 5: Effects of CCR2 and CCL2 inhibition, as well as antibiotic treatment on inflammation and epithelial proliferation.

(A) Expression of chemokine receptors in each macrophage subset. (B) Scheme of the treatment of CCR2 inhibitor or αCCL2. (C-H) Absolute cell numbers of macrophage subset (C-D), normalized gene expression of inflammation-related genes (E-F), and Ki-67 expression in CECs (G-H) from AOM-DSS mice with CCR2 inhibitor or αCCL2 treatment (n = 6-8 per group). Data are represented as mean ± SEM; $p<0.05$ = *; $p<0.01$ = **; $p<0.001$ = ***, student's t test.

Supplemental Figure 6

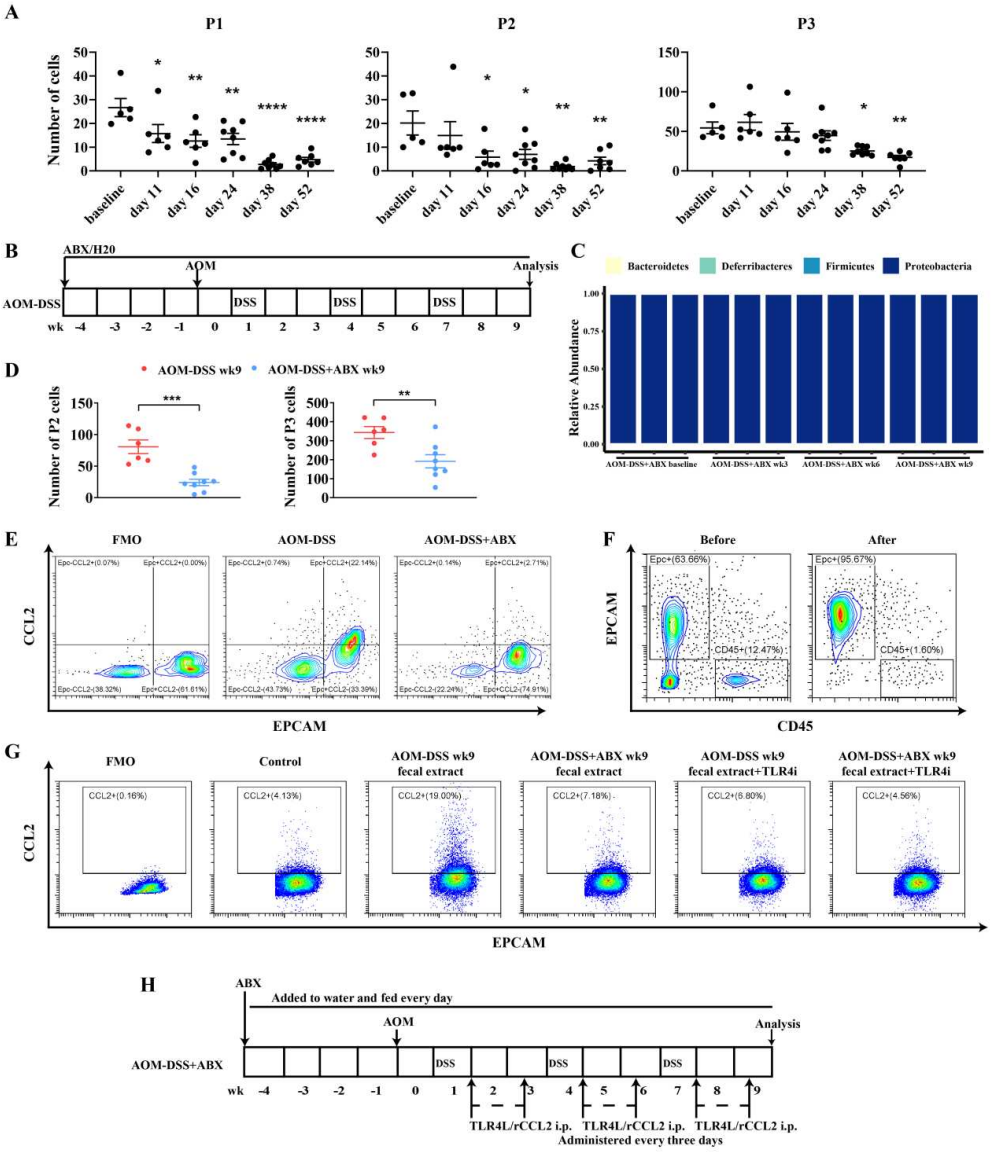

Supplemental Figure 6: The involvement of TLR4 activation in CCL2 up-regulation.

(A) The involvement of the gut microbiota in monocyte-to-macrophage switch. Absolute cell numbers of each macrophage subset (P1, P2 and P3) from the colon of mice that had received antibiotic (ABX) treatment for several days (n = 5-8 for each time-point). Data are represented as mean ± SEM, and each symbol represents one mouse; p<0.05 = *; p<0.01 = **; p<0.001 = ***; p<0.0001 = ****, one-way ANOVA. (B) Scheme of the treatment of vehicle or ABX. Mice were randomly allocated to

each group for ABX versus vehicle (H_2O) treatment, 4 weeks prior to induction with AOM-DSS. (C) The efficacy of ABX was confirmed by 16S rRNA analysis (n = 3 for each time point). (D) Absolute cell numbers of macrophage subset (P2 and P3) in mice treated with H_2O or ABX (AOM-DSS wk9: n = 6; AOM-DSS+ABX wk9: n = 8). $p<0.01$ = **; $p<0.001$ = ***, student's t test. (E) Representative flow cytometry plots of intracellular CCL2 levels in different cell types. (F) Representative flow cytometry plots of epithelial purity analysis. (G) Representative flow cytometry plots of intracellular CCL2 levels in CECs from normal mice treated with fecal extracts, or a combination of TLR4 inhibitor. (H) Schematic showing that ABX-treated AOM-DSS mice additionally received rCCL2 or TLR4 ligand.

Supplemental Figure 7

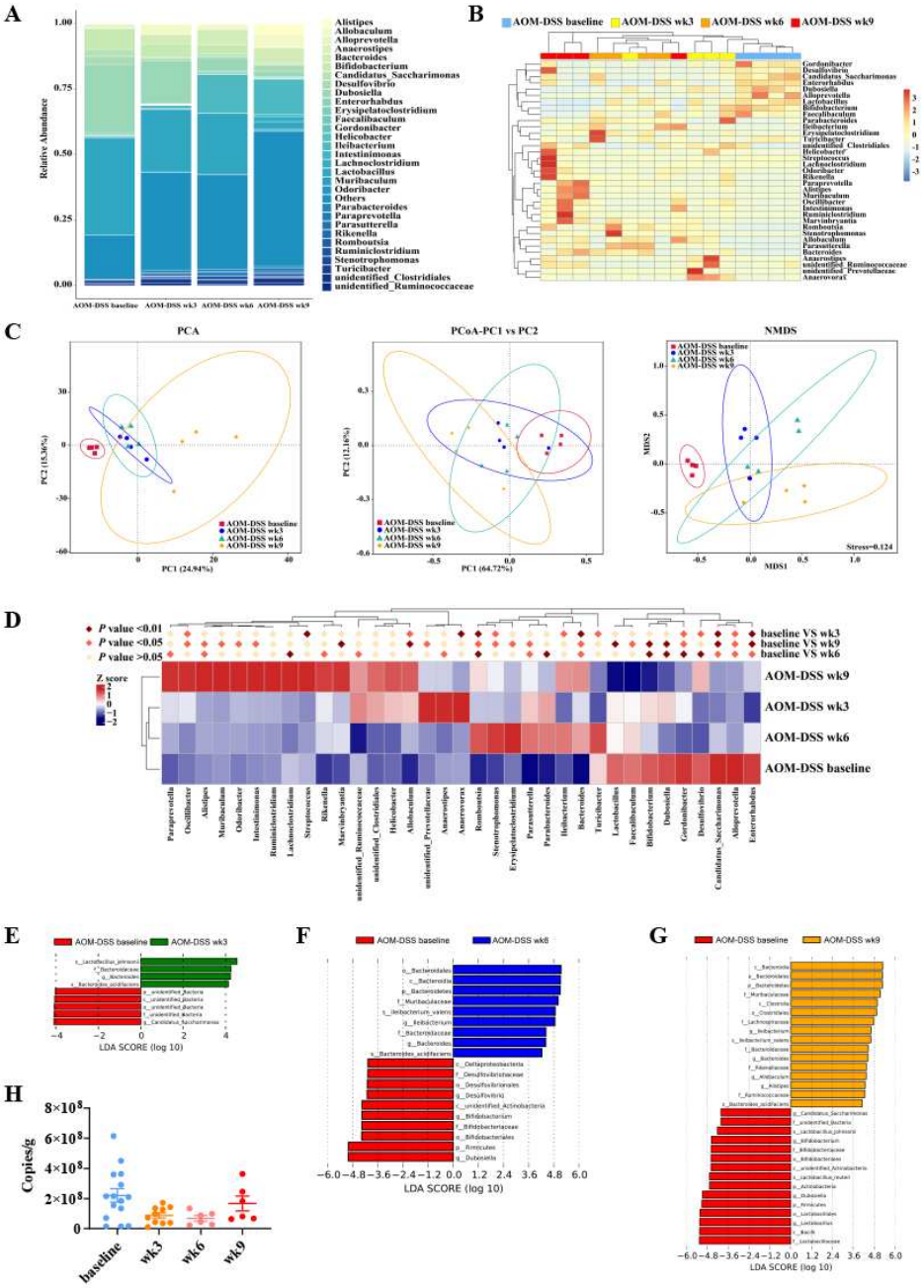

Supplemental Figure 7: Stage-related microbial signatures in colitis-associated tumorigenesis.

(A-B) The relative abundance (genus level) and clustering heatmap (genus level) determined by 16S rRNA sequencing (n = 4 for each time point). (C) The principal component analysis (PCA), principal coordinates analysis (PCoA) of weighted UniFrac distances, and non-metric multidimensional scaling (NMDS) plot throughout

disease progression (n = 4 for each time point). (D) Differentially enriched genera identified by metastat analysis. (E-G) Differentially abundant taxa determined by linear discriminant analysis (LDA). (H) Quantified stool bacterial load throughout disease progression (n = 6-15 for each time point).

Supplemental Figure 8

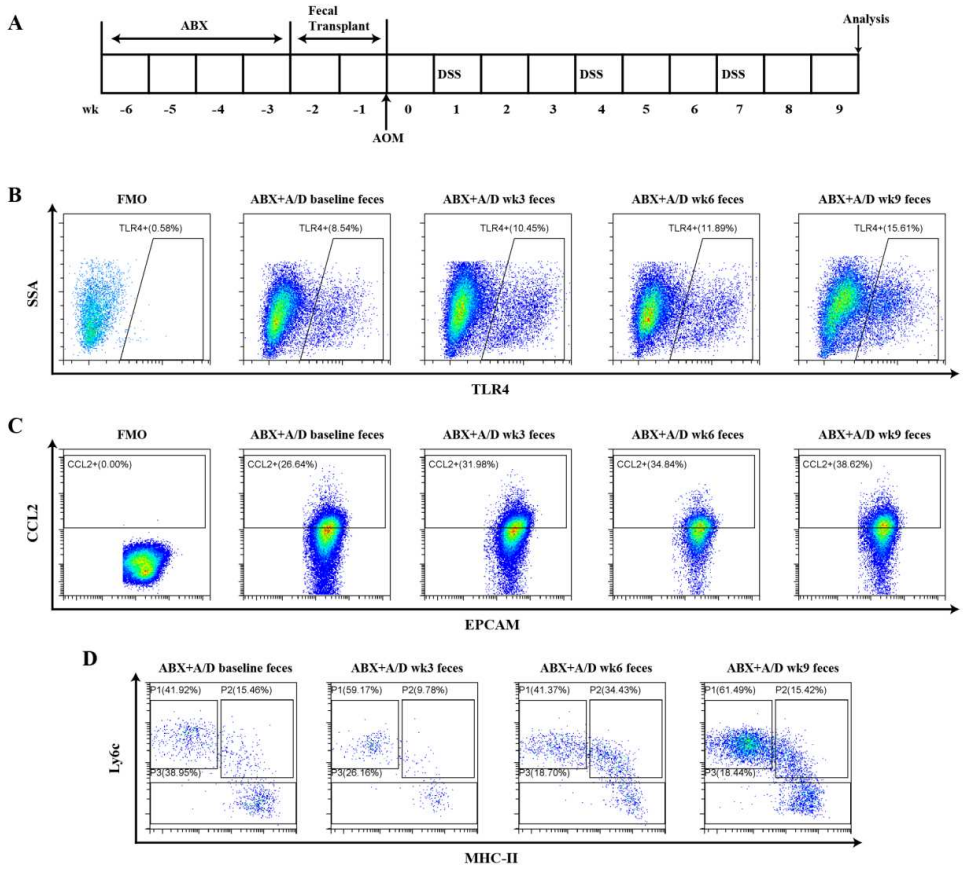

Supplemental Figure 8: The diverse roles of stage-related microbiota in MLM accumulation.

(A) Scheme of fecal transfer experiments. (B-D) Representative flow cytometry plots of TLR4 and CCL2 levels in CECs, and colonic MLM levels from mice repopulated with different stage-related feces. A/D, AOM-DSS.

Supplemental Figure 9

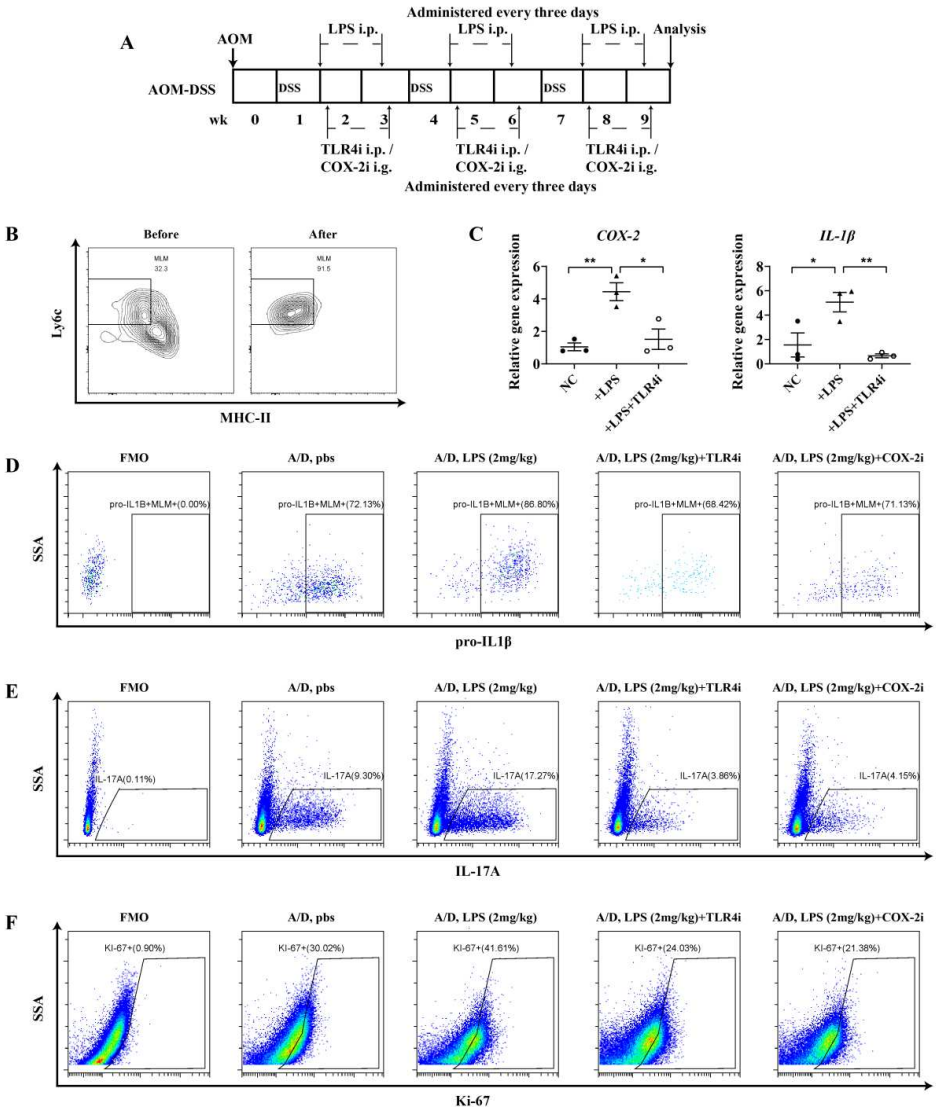

Supplemental Figure 9: TLR4 ligands derived from microbiota induce the accumulation and activation of MLMs.

(A) Scheme of LPS treatment, or a combination of TLR4/COX-2 inhibitor. (B) Representative flow cytometry plots of colonic MLM purity analysis. (C) Sorted colonic MLMs were cultured in the presence of LPS or a combination of TLR4 inhibitor for 36 hours. The leves of *COX-2* and *IL-1β* were determined by qPCR (n = 3 for each group). (D-F) Representative flow cytometry plots of pro-IL1β level in MLMs (D), IL-17A level in $CD4^+$cells (E) and Ki-67 level in CECs (F) from AOM-DSS mice with vehicle or LPS treatment, or a combination of TLR4/COX-2 inhibitor. A/D, AOM-DSS.

Supplemental Figure 10

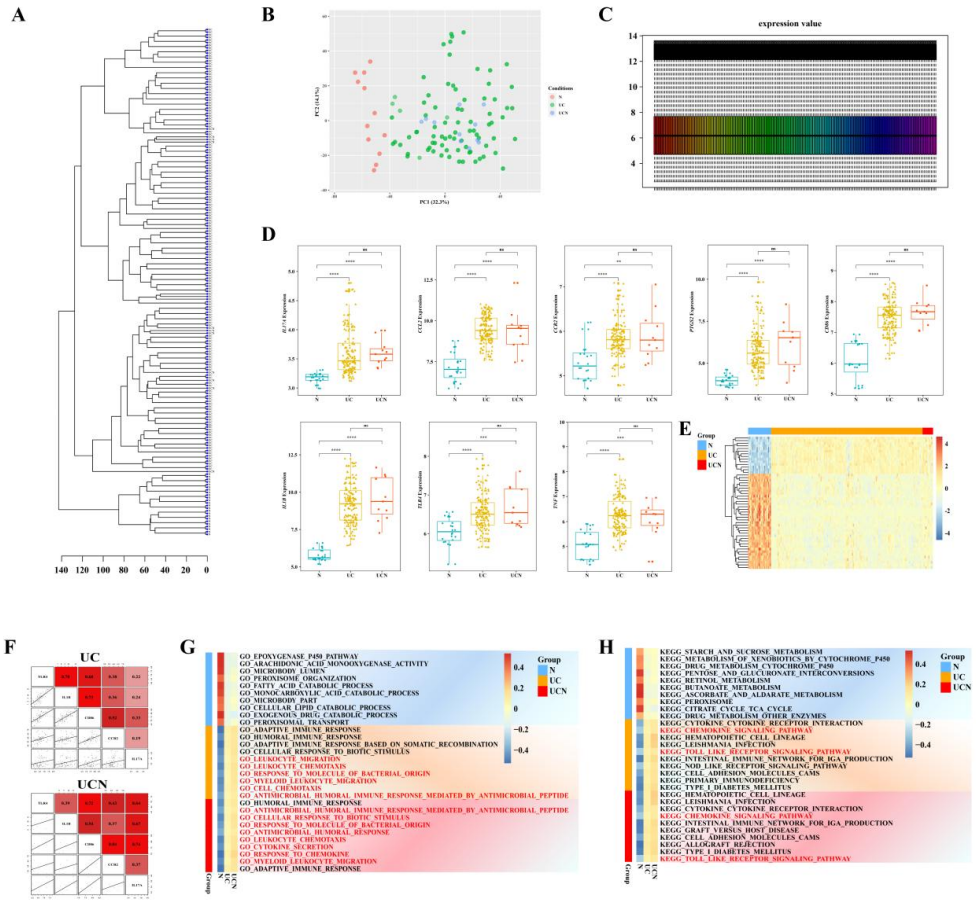

Supplemental Figure 10: Evolving transcriptional signature and immune response during human colitis-associated tumorigenesis

(A-C) Hierarchical clustering, PCA plot and expression values of each series after normalization in merged data sets. (D) Box plots with jittered points showing several differentially expressed genes (DEGs) during disease progression. (E) Heatmap of the top 50 DEGs during colitis-associated carcinogenesis. (F) Correlations among *TLR4*, *IL1B*, *CD86*, *CCR2*, *IL17A* expression in human ulcerative colitis (UC) and ulcerative colitis with neoplasia (UCN) tissues. (G-H) Distinct enriched gene sets between developmental stages using the GSEA analysis.

Supplemental Figure 11

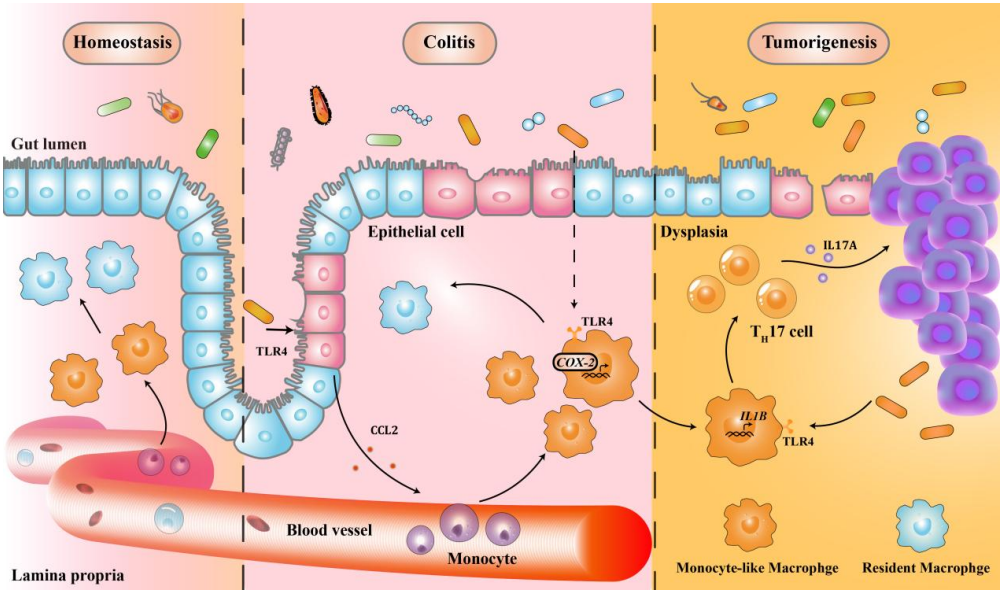

Supplemental Figure 11: Schematic overview of the gut microbiota-immune crosstalk during colitis-associated tumorigenesis. TLR4, Toll-like receptor 4; COX-2, cyclooxygenase-2; Th17 cells, interleukin-17-producing T-helper cells.

Supplemental Table 1: Primers used for qPCR.

Gene	Forward (5' – 3')	Reverse (5' – 3')
mβ-Actin	GGCTGTATTCCCCTCCATCG	CCAGTTGGTAACAATGCCATGT
mCCL1	GGCTGCCGTGTGGATACAG	AGGTGATTTTGAACCCACGTTT
mCCL2	TTAAAAACCTGGATCGGAACCAA	GCATTAGCTTCAGATTTACGGGT
mCCL8	TCTACGCAGTGCTTCTTTGCC	AAGGGGGATCTTCAGCTTTAGTA
mCCR2	ATCCACGGCATACTATCAACATC	CAAGGCTCACCATCATCGTAG
mCCR8	ACGTCACGATGACCGACTACT	CCCAGCACAAACAAGACGC
mCXCR4	GAAGTGGGGTCTGGAGACTAT	TTGCCGACTATGCCAGTCAAG
mTLR1	TGAGGGTCCTGATAATGTCCTAC	AGAGGTCCAAATGCTTGAGGC
mTLR2	GCAAACGCTGTTCTGCTCAG	AGGCGTCTCCCTCTATTGTATT
mTLR3	GTGAGATACAACGTAGCTGACTG	TCCTGCATCCAAGATAGCAAGT
mTLR4	ATGGCATGGCTTACACCACC	GAGGCCAATTTTGTCTCCACA
mTLR5	GCAGGATCATGGCATGTCAAC	ATCTGGGTGAGGTTACAGCCT
mTLR6	TGAGCCAAGACAGAAAACCCA	GGGACATGAGTAAGGTTCCTGTT
mTLR7	ATGTGGACACGGAAGAGACAA	GGTAAGGGTAAGATTGGTGGTG
mNod 1	GAAGGCACCCCATTGGGTT	AATCTCTGCATCTTCGGCTGA
mNod 2	CAGGTCTCCGAGAGGGTACTG	GCTACGGATGAGCCAAATGAAG
mTNF-α	CCCTCACACTCAGATCATCTTCT	GCTACGACGTGGGCTACAG
mIL-1β	GCAACTGTTCCTGAACTCAACT	ATCTTTTGGGGTCCGTCAACT
mIL-12b	TGGTTTGCCATCGTTTTGCTG	ACAGGTGAGGTTCACTGTTTCT
mIL-17A	TTTAACTCCCTTGGCGCAAAA	CTTTCCCTCCGCATTGACAC
mIL-23	ATGCTGGATTGCAGAGCAGTA	ACGGGGCACATTATTTTTAGTCT
mCOX-2	TTCCAATCCATGTCAAAACCGT	AGTCCGGGTACAGTCACACTT

Supplemental Table 3: List of datasets.

Tissues	Enrolled datasets
Normal controls, N (n = 24)	GSM2332098, GSM2332100, GSM2332101, GSM2332102, GSM2332103, GSM2332104, GSM2332105, GSM2332107, GSM2332114, GSM2332115, GSM2332116, GSM2332117, GSM2429455, GSM2429457, GSM2429458, GSM2429459, GSM2429460, GSM2429461, GSM2429462, GSM2429464, GSM2429471, GSM2429472, GSM2429473, GSM2429474
Ulcerative colitis, UC (n = 159)	GSM2332119, GSM2332120, GSM2332121, GSM2332122, GSM2332123, GSM2332124, GSM2332125, GSM2332126, GSM2332127, GSM2332128, GSM2332129, GSM2332130, GSM2332131, GSM2332133, GSM2332134, GSM2332135, GSM2332136, GSM2332137, GSM2332138, GSM2332139, GSM2332140, GSM2332141, GSM2332142, GSM2332143, GSM2332145, GSM2332146, GSM2332147, GSM2332148, GSM2332150, GSM2332152, GSM2332153, GSM2332154, GSM2332155, GSM2332156, GSM2332157, GSM2332158, GSM2332159, GSM2332160, GSM2332161, GSM2332162, GSM2332163, GSM2332164, GSM2332165, GSM2332166, GSM2332167, GSM2332168, GSM2332169, GSM2332170, GSM2332171, GSM2332172, GSM2332173, GSM2332174, GSM2332175, GSM2332176, GSM2332177, GSM2332178, GSM2332179, GSM2332180, GSM2332182, GSM2332183, GSM2332184, GSM2332185, GSM2332186, GSM2332187, GSM2332188, GSM2332191, GSM2332192, GSM2332193, GSM2332194, GSM2332195, GSM2332197, GSM2332198, GSM2332199, GSM2332200, GSM2332201, GSM2332202, GSM2332203, GSM2332204, GSM2332205, GSM915451, GSM915452, GSM915453, GSM2429346, GSM2429347, GSM2429348, GSM2429349, GSM2429350, GSM2429351, GSM2429352, GSM2429353, GSM2429354, GSM2429355, GSM2429356, GSM2429357, GSM2429358, GSM2429359, GSM2429360, GSM2429361, GSM2429362, GSM2429363, GSM2429364, GSM2429365, GSM2429366, GSM2429367, GSM2429368, GSM2429369, GSM2429370, GSM2429371, GSM2429372, GSM2429373, GSM2429374, GSM2429375, GSM2429376, GSM2429378, GSM2429379, GSM2429380, GSM2429381, GSM2429383, GSM2429385, GSM2429386, GSM2429387, GSM2429388, GSM2429389, GSM2429390, GSM2429391, GSM2429392, GSM2429393, GSM2429395, GSM2429396, GSM2429397, GSM2429398, GSM2429399, GSM2429400, GSM2429401, GSM2429402, GSM2429403, GSM2429404, GSM2429476, GSM2429477, GSM2429478, GSM2429481, GSM2429482, GSM2429484, GSM2429485, GSM2429486, GSM2429487, GSM2429488, GSM2429489, GSM2429490, GSM2429492, GSM2429495, GSM2429496, GSM2429497, GSM2429498, GSM2429499, GSM2429500, GSM2429501, GSM2429502, GSM2429503
Ulcerative colitis with neoplasia, UCN (n = 11)	GSM915460, GSM915461, GSM915462, GSM915463, GSM915464, GSM915465, GSM915466, GSM915467, GSM915468, GSM915469, GSM915470